International Journal of Radiology and Diagnostic Imaging

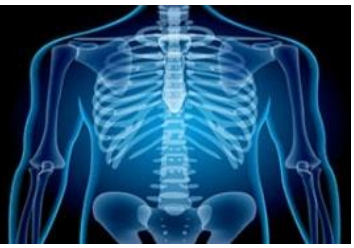

E-ISSN: 2664-4444
P-ISSN: 2664-4436
www.radiologypaper.com
IJRDI 2023; 6(3): 123-132
Received: 02-07-2023
Accepted: 07-08-2023

Amira M Abdelmaksoud
Department of Radiodiagnosis, Faculty of Medicine, Tanta University, Tanta, Egypt

Dina M Mohamad
Department of Radiodiagnosis, Faculty of Medicine, Tanta University, Tanta, Egypt

Rasha M Dawoud
Department of Radiodiagnosis, Faculty of Medicine, Tanta University, Tanta, Egypt

Lina T Hablas
Department of Radiodiagnosis, Faculty of Medicine, Tanta University, Tanta, Egypt

Corresponding Author:
Amira M Abdelmaksoud
Department of Radiodiagnosis, Faculty of Medicine, Tanta University, Tanta, Egypt

Diagnostic efficiency of anatomic features measured by 320- slice multi-detector computed tomography angiography in evaluating the severity of aortic coarctation

Amira M Abdelmaksoud, Dina M Mohamad, Rasha M Dawoud and Lina T Hablas

DOI: https://doi.org/10.33545/26644436.2023.v6.i3b.352

Abstract
Background: Coarctation of the aorta is the most frequent congenital anomaly of the thoracic aorta. It's severity depend on pressure gradient across coarctation site that has been shown to be correlated with antomical structure alternation in the aorta. The aim of this work was to quantify the extent of coarctation of the aorta by utilizing the anatomical characteristics determined on 320 slice multi-detector computed tomography angiography.
Methods: This prospective work was performed on 50 individuals (29 males and 21 females) aged from 1 day to 29 years old, with clinical criteria of patients known and suspected aortic coarctation or presented with other cardiac anomalies by echocardiography. By computed tomography the diameter of aorta at coarctation site and at diaphragm were measured, four ratios were calculated; coarctation area / body surface area ratio, diameter of aortic coarctation / diameter of descending aorta ratio, coarctation diameter / height ratio and coarctation diameter / weight ratio.
Results: By statistical correlation, multi-slice CT could classify the severity of aortic coarctation by indexing aortic coarctation area to patient body surface area with sensitivity 95.65%, specificity 92.86% and cut off value ≤23.8 mm^2.
Conclusions: The anatomical characteristics derived from computed tomography angiography can assess the extent of aortic coarctation, suggesting that it is important to take into account both the anatomical alterations at the CoA sites and the patient's development.

Keywords: Anatomic parameters, aortic coarctation, congenital heart diseases, multi- detector computed tomography angiography

Introduction

Globally, the prevalence of congenital heart disease (CHD) is close to 9 per 1000 newborns. Aortic coarctation is a frequent kind of congenital cardiovascular disorder that affects 1 in every 3000 live births and is diagnosed in 5-8% individuals with congenital cardiovascular disorders. It may manifest alone or in conjunction with a number of other heart and vascular defects, including ventricular septal defect, bicuspid aortic valve, patent ductus arteriosus, and aortic arch hypoplasia [1, 3].

A discrete or extended stenosis in the aorta, often near the isthmus, with numerous levels of severity is what is known as coarctation of the aorta. Hypertension of the upper body and a decreased supply of blood to the lower limbs are the results of the increased flow resistance that develops. In order to determine if a repair is necessary and if the repair was effective or not, the pressure gradient, the differences in pressure across the coarctation, is often employed [4].

To choose the optimal course of therapy for each patient, a thorough morphological and functioning evaluation of the aortic arch is necessary. Imaging is frequently required for aortic coarctation diagnosis, as is measuring of the pressure gradient across the coarctation to assess its severity. Accurate measurements may be made using an oximetry run acquired during cardiac catheterization. In several clinical instances, however, non-invasive imaging such as multi-detector CT angiography with multi-planar and 3-D methods is the approach of decision, prior to or instead of invasive angiography evaluation.

Cardiac catheterization is no longer employed in these instances. Whenever the pressure gradient at rest is larger than 20 mmHg, surgical procedures are necessary. Therefore, for efficient therapy planning, knowledge of the degree of aortic coarctation is essential [5, 7].

It was recently demonstrated that the pressure gradient brought on by coarctation corresponds to changes in the aorta's anatomical structure, Anatomical variables by themselves, however, might be misleading, Therefore, a trustworthy evaluation of the degree of coarctation might be accomplished by combining both physical characteristics and demographic data representing body development (such as height, age, and weight) [8, 9].

The aim of this work was to quantify the extent of the aortic coarctation by using the anatomical features measured on 320 slice multi-detector computed tomography angiography.

Materials and Methods

This prospective work was performed on 50 individuals (29 males and 21 females) aged from 1 day to 29 years old, with clinical criteria of patients known or strongly suspected aortic coarctation in echocardiography, presented with other cardiac anomalies by echocardiography and computed tomography angiography with incidentally discovered aortic coarctation, patients who undergo surgical intervention with suspected re-coarctation.

The study was done from January 2022 and January 2023 following Tanta University Hospitals, Egypt's medical ethics committee has approved. The participant's relatives provided written permission after being properly briefed.

Exclusion criteria were patients with no previous echocardiographic examination, history of renal problems (serum creatinine higher than 1.5 mg /dL) or severe allergic response to iodinated-contrast media.

Before making the proper care plans, every participant who had aortic coarctation suspected or confirmed had MSCT angiography of their hearts and great vessels to verify the diagnosis or resolve particular anatomic problems generated by equivocal echocardiogram findings.

Parents were properly questioned about their child's history, and patient demographic information, such as height, age, weight, and body surface area (BSA), was also gathered.

Preparing the patient: A right upper limb vein (38 instances) or a lower limb peripheral vein (12 cases) were both used to insert an intravenous cannula. Chloral hydrate (n=44; 50-100 mg/kg; maximum dosage, 2000 mg) or intravenous midazolam (n=2) (0.05-0.1 mg/kg) were used to sedate the 46 individuals below the age of 4 years. Elderly patients (n=4) were capable of totally suspend breathing and were responding effectively to verbal reassurance.

CT Examination' Technique: The Aquilion One, a 320-row multidetector CT scanner from Toshiba Medical Systems in Otawara, Japan, was used to scan the patients.

Following using alcohol to prepare the skin, ECG electrodes were placed on the chest wall. The ECG trace was observed to confirm that the R wave, which served as the scan trigger, had a satisfactory amplitude.

A scanogram (frontal & lateral views) was acquired. Non-ionic, non-diluted contrast substance (Omnipaque 300, Nycomed, Amersham) has been administered via the peripherally introduced IV cannula utilising dual-syringe mechanical power injector (Stellant D, Medrad, Indianola, PA, USA) via flow rate 1-1.5 ml/sec raised to 3 ml/sec in elder children and 5-6 ml/sec in adults. The amount of contrast was estimated based on body weight, with a 2 ml/kg maximum dosage. All scans were carried out in a cranio-caudal orientation using weight-based CT parameters. A single-phase retrospective ECG gated CTA volume scan was used on the participants, with a rotation time of 0.35 seconds and tube voltages starting at 80 kV and increasing to 100-120 kV for two elder children and adults. prior to the inspection was over, the image's quality was assessed. Following the examination, the dose-length product (DLP) was acquired for the purpose of evaluating the radiation dosage, and the participant remained under monitoring until the sedation had subsided.

No extravasation or response of contrast, in any way, ever happened throughout the multi-slice CT angiography evaluation.

In a slice with a thickness of 0.5 mm, full volumes were reconstituted. Multi-detector CT (MDCT) scan after processing was carried out using a specialist workstation (Vitrea Fx, vital imaging, USA). Heart abnormalities were visualised using maximum intensity projections (MIP), multiplanar (MPR), 3-D volume rendering (VR), and curved planar reformations (CPR).

Reformation planes: a line was projected onto one of the transverse sections to ensure that the resulting MPR pictures were parallel to the projected line and perpendicular to the transverse plane. For measuring vessels precisely, thin MPR pictures are employed.

The size of the primary pulmonary arteries and thoracic aorta has been assessed using curved planar imaging.

VR acquired during bone removal. The volume-rendering approach proved effective for showing structures that run oblique or parallel to the transverse plane, in addition, for showing how the extra-cardiac arteries are related to one another and for visualising the pulmonary and systemic venous drainage. It also serves as the surgery's route plan.

The assimilation of sections in a volume slab may sometimes provide a clearer view of peripheral arteries and airways in CT scans, which are taken at their standard section thickness and then merged to form "slabs" that are thicker in comparison.

Image analysis

The narrowest diameter of aorta at coarctation site and the aortic diameter at diaphragm were measured.

Four ratios were calculated: coarctation area / body surface area (BSA) ratio, diameter of aortic coarctation / diameter of descending aorta ratio (CoA / DAo), coarctation diameter / height ratio, coarctation diameter / weight ratio. The anatomic and segmental/sequential approaches were used to evaluate the images, excluding other cardiac abnormalities.

Assessments: Heart: Size and shape of the heart chambers, the existence of intra-cardiac mass or thrombus or effusions in the pericardium, interatrial septum: detection if intact or with ASD (type, size), interventricular septum: detection if intact or with VSD (type, size), and ventriculo-arterial concordance/discordance, atrio-ventricular concordance / discordance.

Aortaz: Ormal, tiny, enlarged, or right or left ventricle.

Left- or right-sided, tiny or big, interrupted, double, or hypoplastic, branched out, typical or bovine arch, abnormal right subclavian artery, or abnormal left subclavian artery are all aspects of the aortic arch.

Origin, typical, dilated, tiny, atretic, confluence are all aspects of the pulmonary arteries. dilated bronchial arteries or significant pulmonary-collaterals. Size and drainage abnormalities of the pulmonary veins. Systemic venous drainage: draining from the left superior venae cavae and the inferior venae cavae. Coronary arteries: correctly or incorrectly evaluated, including their origin, course, and anomalies. Each participant's dose-length product was noted. The findings of the dosage-length product multiplied by the conversion factor were utilized to calculate the cardiac CTA effective dose [10, 11].

The CTDI phantom was 36 cm in size. varied age groups have varied specific dosage length-product conversion coefficients: A conversion coefficient of 0.039mSv/(mGy-cm) is applied to children under the age of four; Between 4 months and 1 year the conversion coefficient is 0.026 mSv/(mGy-cm), 0.018 mSv/(mGy-cm) is applied to children between the ages of one and six; and 0.014 Sv/(mGy-cm) is applied to children above the age of six [12, 13].

Statistical analysis: Statistical analysis was done by SPSS V.20. Quantitative variables were presented as mean and standard deviation (SD), range (minimum and maximum) and median. Qualitative variables were presented as number and percentage (%). For categorical variables, Chi-square test was used. Pearson correlation between CoA diameter, AAD (Aorta at diaphragm diameter) and patient's demographic information and anatomical features between the mild CoA and severe CoA groups was also done. Receiver-operating characteristic curve (ROC) was performed to determine the cutoff value of coarctation area / BSA, coarctation diameter/ height and coarctation diameter/ weight to predict severity of aortic coarctation a two tailed P value < 0.05 was considered significant.

Results

Among all 50 patients, aortic coarctation was diagnosed correctly by MSCT through axial, multiplanar and three-dimensional images with 100% sensitivity. Echocardiography failed in the accurate diagnosis of coarctation of aorta in 13 cases with sensitivity 74%.

Table 1: Criteria of age & gender, presenting symptoms, Percentage of collaterals detected by MSCT of 50 cases with coarctation of aorta. Detection of associated intracardiac and extra-cardiac anomalies by MSCT. Number & percentage of cases of aortic coarctation detected by echocardiography & MSCT

Parameters		No.
Sex	Male	29 (58%)
	Female	21 (42%)
Age	Less than month	19 (38%)
	1 month - ≤ 4months	16 (32%)
	4 month - ≤ 12 months	7 (14%)
	12 months - ≤ 4 years	4 (8%)
	More than 4 years	4 (8%)
	Median (IQR)	1.67 (0.70-5.0)
Presenting symptoms		
Cyanosis		16 (32%)
Murmur		14 (28%)
Dyspnea		15 (30%)
Headache		3 (6%)
Hypertension		2 (4%)
Palpitation		3 (6%)
Poor feeding		3 (6%)
Associated intra-cardiac anomaly diagnosed by MSCT		
ASD		10 (20%)
VSD		5 (10%)
ASD & VSD		13 (26%)
Patent foramen ovale.		2 (4%)
Ventricular hypertrophy		22 (44%)
Dilated atria		9 (18%)
DORV		2 (4%)
None		18 (36%)
Associated extra-cardiac anomaly diagnosed by MSCT		
Patent ductus arteriosus		18 (36%)
Arch hypoplasia		10 (20%)
Persistent left SVC		8 (16%)
Hypoplastic ascending aorta		2 (4%)
Aortic arch branching variants		3 (6%)
TGA		1 (2%)
Dilated pulmonary artery		21 (42%)
Situs ambiguous (polysplenia)		2 (4%)
None		15 (30%)
Collaterals by MSCT	Absent	42 (84%)
	Present	8 (16%)
Detection of coarctation	Echo	37 (74%)
	MSCT	50 (100%)

Data are presented as number (percentage), MSCT: Multi-slice computed tomography, IQR: Interquartile range, ASD: Atrial septal defect, VSD: ventricular septal defect, DORV: double outlet right ventricle, TGA: transposition of great vessels, SVC: Superior vena cava.

Demographic characteristics were adjusted to the obtained coarctation diameter to validate their applicability in classifying coarctation severity.

Table 2: Demographic data, classification of the suitable cases according to severity of coarctation by echo, aortic measurements of the suitable cases (n = 37) as regard coarctation diameter and area, Descriptive statistics of indexed anatomic variables to aortic measurements between mild & severe coarctation patients, Mean absorbed and effective radiation doses in different age groups of the study population

Severity of coarctation by echo		No	P
Mild (Pressure gradient < 20 mmHg)		14 (37.8%)	-
Severe (Pressure gradient > 20 mmHg)		23 (62.2%)	-
Sex	Male	24 (%)	-
	Female	13 (%)	-
Age (months)		1.33 (0.67-4.0)	-
Height (cm)		57.0 (49.0-62.0)	-
Weight (Kg)		4.30 (3.70-5.60)	-
BSA (mm2)		0.25 (0.22-0.30)	-
Coarctation area (mm^2)		5.0(2.20-4.0)	-
Coarctation diameter (mm)		3.0(4.0-8.0)	-
Severity by echo			-
Coarctation area / BSA	Mild< 20 mmHg (n = 14)	35.17±11.52	<0.001*
	Severe> 20 mmHg (n = 23)	15.61±5.91	
Coarctation diameter/ height	Mild< 20 mmHg (n = 14)	0.06	<0.001*
	Severe> 20 mmHg (n = 23)	0.04	
Coarctation diameter/ Dao	Mild< 20 mmHg (n = 14)	0.56±0.07	<0.001*
	Severe> 20 mmHg (n = 23)	0.37±0.11	
Coarctation diameter/ weight	Mild< 20 mmHg (n = 14)	0.78±0.23	<0.001*
	Severe> 20 mmHg (n = 23)	0.50±0.20	
Coarctation diameter/ age	Mild< 20 mmHg (n = 14)	2.38	0.066
	Severe> 20 mmHg (n = 23)	1.35	
Radiation dose evaluation			-
< 4 months N=33	Dose length produce (mGy-cm)	75.97±30.85	
	Effective dose (mSv)	2.91±1.19	
≥ 4 - < 12 months N=9	Dose length produce (mGy-cm)	115.26±19.49	
	Effective dose (mSv)	3.25±0.40	
≥12 months - < 6 years N=4	Dose length produce (mGy-cm)	164.52±17.09	
	Effective dose (mSv)	2.81±0.34	
≥ 6 years N=4	Dose length produce (mGy-cm)	1697.50±1415.16	
	Effective dose (mSv)	23.76±19.82	
Total N=50	Dose length produce (mGy-cm)	219.85±563.70	-
	Effective dose (mSv)	4.63±7.58	

Data are presented as mean ±SD or number (percentage) or median IQR, BSA: body surface area statistically significant at $p \leq 0.05$

A ROC analysis was performed for each set of morphometric and hemodynamic data. A p-value of ≤ 0.05 was statistically significant. It revealed sensitivity 95.65%, specificity 92.86% and AUC of 0.994 using CoA area / BSA with cut off value ≤23.8 mm^2.

And by using CoA / patient height, it revealed sensitivity 95.65%, specificity 78.57% and AUC of 0.972 with cut off value ≤ 0.05 mm. While using CoA / patient weight it revealed sensitivity 91.30%, specificity 85.71% and AUC of 0.891 with cut off value ≤ 0.66 mm.

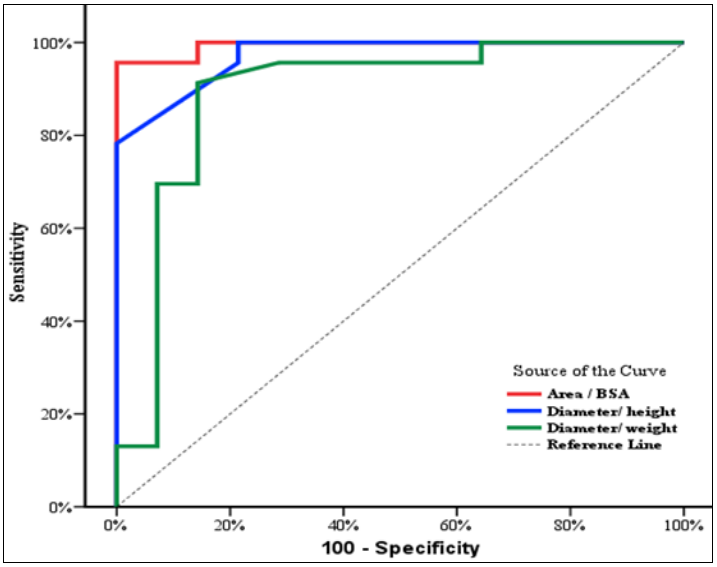

Fig 1: ROC curve for coarctation area / BSA, coarctation diameter/ height and coarctation diameter/ weight to predict severity of aortic coarctation

Case 1

Female patient aged 11 days with height of 47 cm, weight of 2.5 Kg & BSA of 0.18 m^2 and clinical history of dyspnea at rest. Echocardiography was done and showed focal aortic narrowing just beyond the site of PDA, univentricular heart and normal relationship of great vessels, then referred for further assessment of aortic anomaly.

Cardiac CT angiography findings: Aorta arises posterior to MPA from the morphological RV, hypoplastic ascending aorta measures 1.8 mm, left sided aortic arch with normal branching pattern showing mild post ductal focal aortic arch coarctation, coarctation diameter = 3 mm & Coarctation area = 6 mm^2.Aneurysmal dilated MPA that arises normally from the morphological RV; main pulmonary artery measures 19 mm, right pulmonary artery measures 6 mm, left pulmonary artery measures 5.5 mm. Heart: situs solitus with levocardia, atrioventricular connection: Only one single ventricular chamber is identified connected to right atrium through single atrioventricular valve, ventriculo-arterial connection: DORV, markedly dilated right atrium and morphological right ventricle with atretic left ventricle, intact inter-atrial septum. Sizable tubular PDA connecting aortic isthmus with MPA; aortic end measures 3.2 mm & pulmonary end measures 4.5 mm Systemic veins: Superior vena cava and Inferior vena cava drain normally into right atrium. From our results coarctation area / body surface area =33.3, coarctation diameter/ height =.06 & coarctation diameter/ weight = 1.2, so considered as mild case. Figure 2

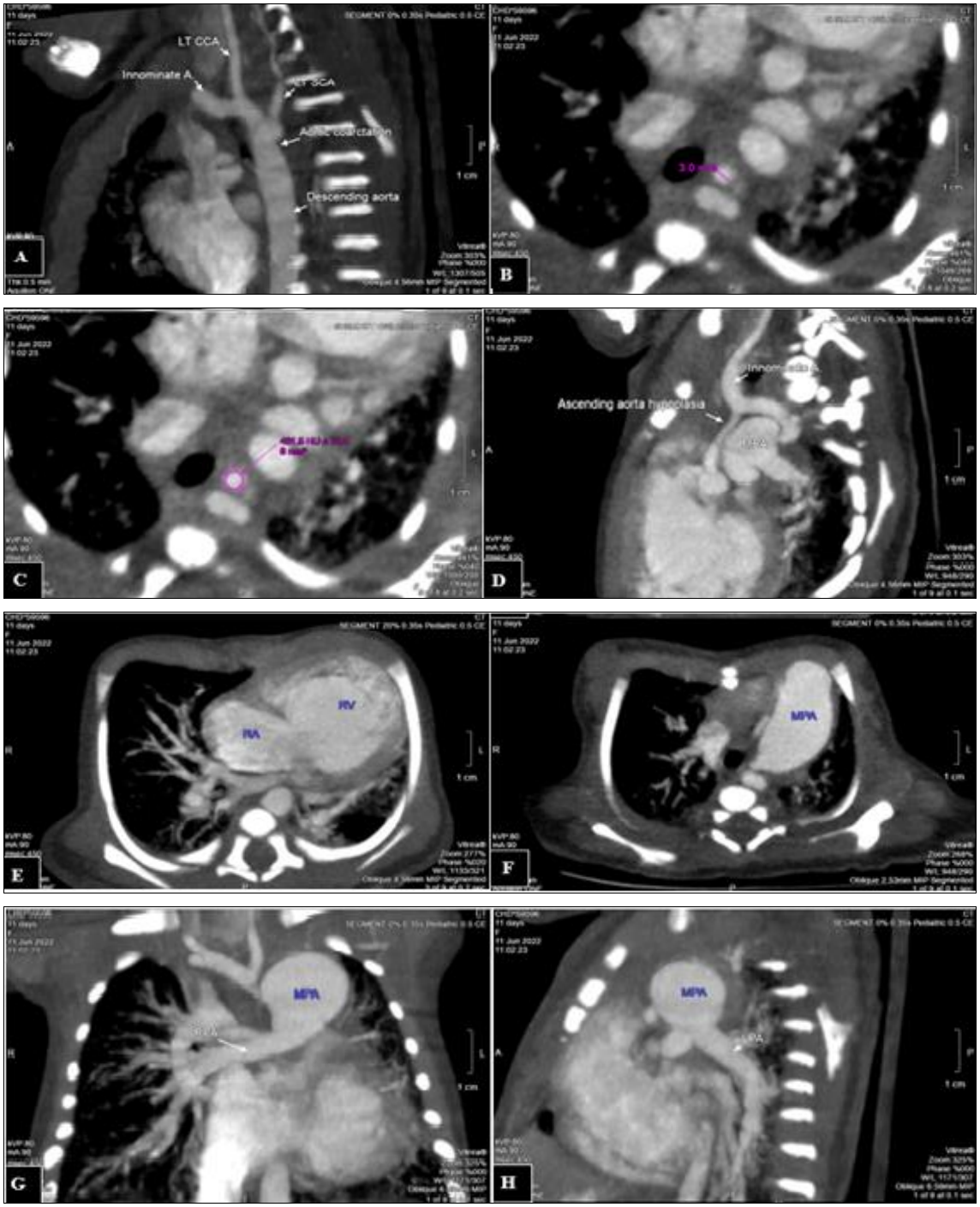

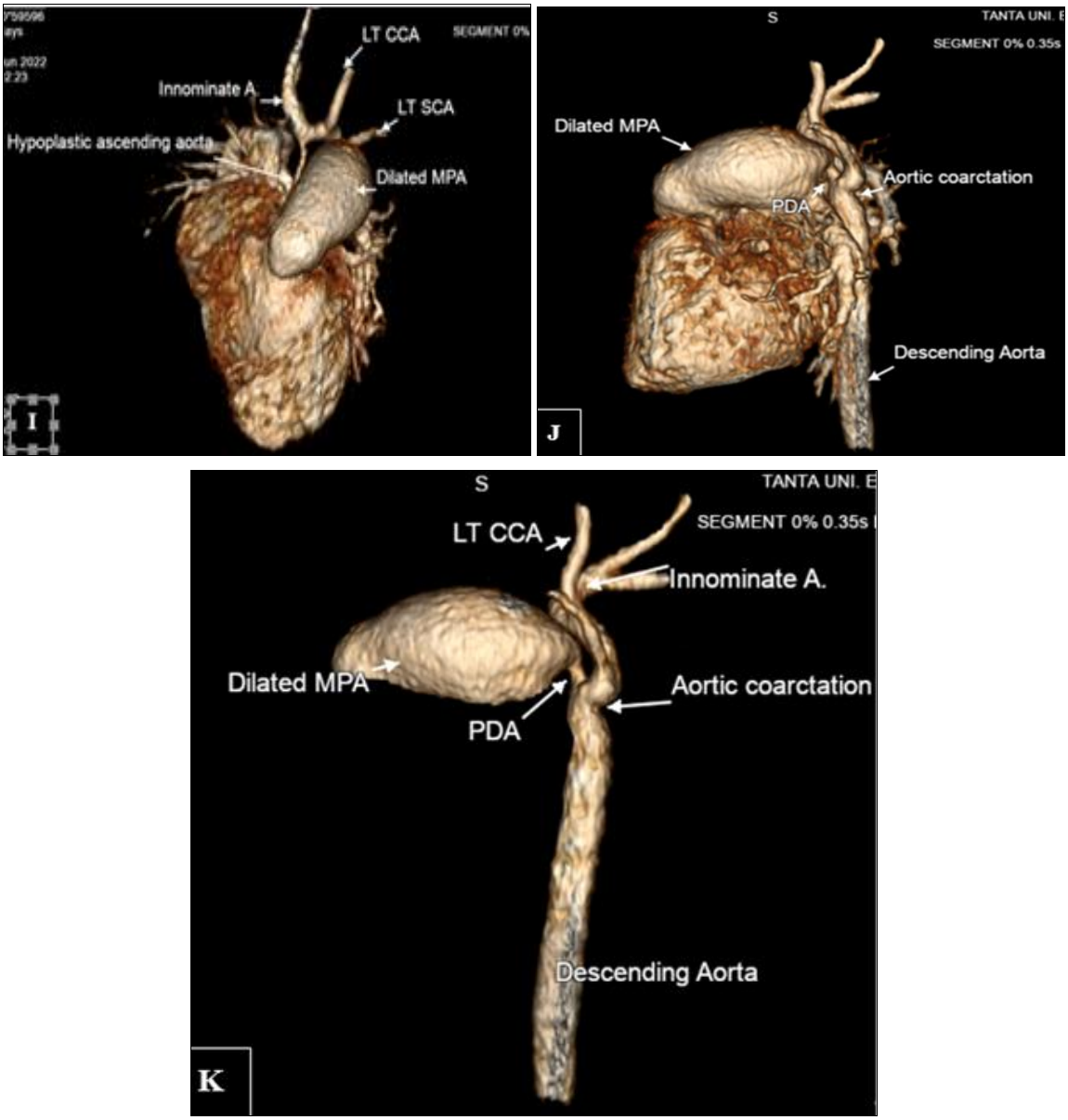

Fig 2: Oblique MPR images with MIP showing mild post ductal aortic coarctation (A), aortic coarctation diameter of 3 mm (B), aortic coarctation area of 6 mm^2 (C). D) hypoplastic ascending aorta, E) single ventricular chamber. aneurysmally dilated main pulmonary artery (F), dilated both right and left pulmonary arteries (G & H). 3D-Volume rendering MSCT images showing hypoplastic ascending aorta (I), PDA with post ductal aortic coarctation and aneurysmally dilated MPA (J & K)

Case 2

Male patient aged 20 days with height of 50 cm, weight of 4.3 Kg & BSA of 0.24 m^2 and clinical history of cyanosis while feeding. Echocardiography was done and showed diffuse hypoplasia of aortic arch with focal aortic narrowing, small PDA, two muscular VSDs and mildly dilated LV, then referred for further assessment of aortic anomaly.

Cardiac CT angiography findings: Aorta arises anteriorly and to the right side of MPA from the morphological RV, left sided aortic arch with showing long segment of tubular hypoplasia distal to innominate artery down to aortic isthmus with severe focal aortic coarctation at aortic isthmus itself, coarctation diameter = 2.3 mm & Coarctation area = 4 mm^2, left vertebral artery arise directly form aortic arch (normal variant). MPA arises posteriorly to left side of aorta from the morphological LV with dilated caliber, main pulmonary artery measures 18 mm, right pulmonary artery measures 7.5 mm, left pulmonary artery measures 7 mm. Heart: Situs solitus with levocardia, atrioventricular connection: concordant, ventriculo-arterial connection: Discordant (TGA), large muscular VSD measures 32 x 15 mm, intact inter-atrial septum, markedly dilated right ventricle. Funnel shaped PDA connecting aortic isthmus with MPA; aortic end measures 3.3 mm & pulmonary end measures 2 mm. Systemic veins: SVC and IVC drains normally into right atrium. From our results coarctation area / body surface area =16.6, coarctation diameter/ height = .04, coarctation diameter/ weight = .53, so considered as severe case. Figure 3

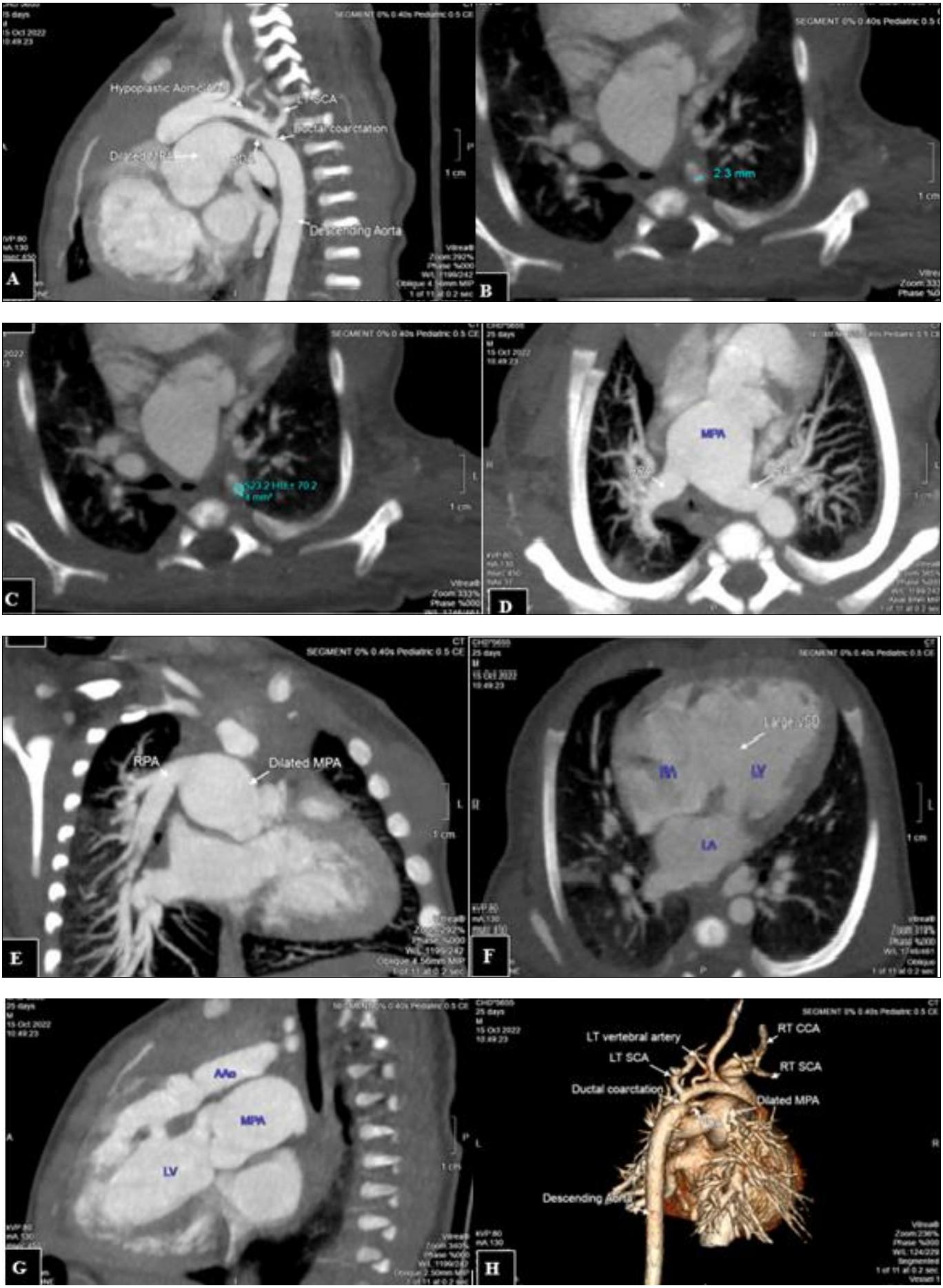
Hypoplastic Aortic arch
LT SCA
Ductal coarctation
Descending Aorta
2.3 mm
MPA
RPA
Dilated MPA
RV
LV
LA
AAo
RT CCA
LT vertebral artery
LT SCA
RT SCA
Ductal coarctation
Dilated MPA
Descending Aorta
A
B
C
D
E
F
G
H

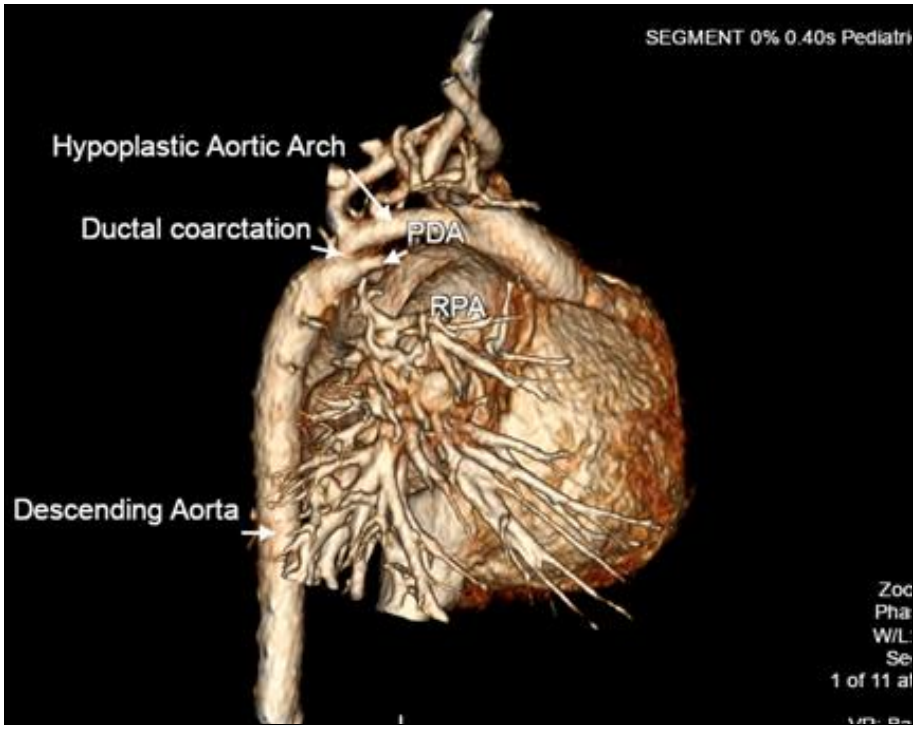

Fig 3: Oblique MPR images with MIP showing severe form of aortic coarctation, PDA & dilated MPA (A), aortic coarctation diameter of 2.3 mm (B), aortic coarctation area of 4 mm^2 (C). Dilated main pulmonary artery and its branches D & E), Oblique MPR images (F) four chambers view showing large VSD, (G) showing transposition of aorta and MPA. H& I) 3D-Volume rendering MSCT images showing hypoplastic aortic arch with ductal aortic coarctation and PDA with dilated MPA. Note left vertebral artery arise directly form aortic arch (H)

Discussion

A localised or long-segment constriction of the aorta, often at the aortic isthmus, is known as coarctation of the aorta (CoA). It typically occurs alongside with other cardiac anomalies. Long-term consequences might include left ventricular failure, arterial hypertension, or the development of aortic and cerebral aneurysms [14].

ECG gated acquisition was employed in the present investigation using a 320-slice scanner with a low dose of radiation protocol of 80 kV in 46 individuals and 100 kV in 4 elderly individuals with automated mAs adaptation. In a subsequent investigation, Shehata *et al*. used CT with 128 detectors with retrospectively ECG-gating, and this result was substantially decreased [15]. Showed an additional dosage decrease to 0.8 ±0.39mSv, which they attribute to the use of prospectively ECG gating. In addition, Chandrashekhar *et al*. [16] noted that just 20 children in their research group had access to the radiation dosage for cardiac catheter angiography, and that this dose ranged from 4.2 mSv to 12 mSv, an amount that is significantly greater than that required for 64 MDCT.

Based on the recent research, in regards to image interpretations, axial, multiplanar, and 3D pictures had 100% sensitivity in properly diagnosing all coarctations. The sensitivity of MDCT angiography for the diagnosis of coarctation of the aorta is 100%, and that's greater than that of Doppler echocardiography (74%), in 13 cases where echocardiography failed to accurately diagnose coarctation of the aorta, that was diagnosed afterwards via MDCT.

While Omnia *et al*. [17] found that 100% of coarctations could be accurately detected by multiplanar and 3D imaging, which was a better sensitivity than Doppler echocardiography (91%). ECG-gated MDCT angiography, according to Goo *et al*. [18], may effectively display the anatomical specifics and shape of the intracardiac abnormality. Interatrial and interventricular septal defects may be seen clearly using MDCT angiography. More care must be used when diagnosing ASDs with less than 3 mm, however. Lesions may go undetected on CT scans because to the interatrial septum's thin appearance, particularly in close proximity of the fossa ovalis. Kim *et al*., [19] found that 4.6% of patients had atrioventricular septal defect. In present study five cases had ventricular septal defect (10%), 10 cases had atrial septal defect (20%) and 13 cases (26%) had combined ventricular and atrial septal defects were correctly diagnosed by MDCT angiography. In our study using MDCT angiography (44%) cases were correctly diagnosed with ventricular hypertrophy, among them (26%) had left ventricular hypertrophy, (12%) had right ventricular hypertrophy and (6%) had biventricular hypertrophy, while in Sendzikaite. S *et al*., [20] study, left ventricular hypertrophy was diagnosed in 32.2% patients. Wu *et al*., [21] found that about 2% had double outlet of right ventricular (DORV), while in this study, DORV was found in 2 cases (4%).

In our study, CoA was correlated with further extracardiac vascular anomalies in (70%). MDCT angiography correctly diagnosed the extra-cardiac vascular anomalies starting from patent ductus arteriosus in (36%) while Dijkema *et al*., [22] found that 21% of the studied group had patent ductus arteriosus and Zhao *et al*., [23] found that about 54% had PDA, also it was found that aortic arch hypoplasia was in (20%) while Dijkema *et al.* [22] found that 21% of the studied group had hypoplastic aortic arch.

As regard persistent left superior vena cava Teo.*et al*., [24] found that about 4.2% had persistent left SVC, while in this study, there was persistent left superior vena cava in (16%).

As regard pulmonary artery anomalies, (2%) was diagnosed

as transposition of great vessels TGA in the present study, also found 2 cases with polysplenia as a part of situs ambiguous and 2 cases with hypoplastic ascending aorta, while Kim *et al*., [19] found that 6.9% of patients had transposition of great arteries.

In the current study, Collateral vessel formation was demonstrated in 16% of cases (8/50). This lower than Omnia *et al*., [17] who found 16 cases (57%) with collateral vessel formation (16/28).

Every patient's severity of aortic coarctation was categorized as mild (14 instances) and severe (23 cases) based on the pressure gradient determined by echocardiography. By contrasting the anatomic characteristics of individuals who had and did not have PDA, Pulmonary hypertension, and VSD, Yu. *et al*. [8] investigated the possibility that the alteration in pressure gradient brought on by additional conditions may not be sufficiently substantial to affect the evaluation of severity of aortic coarctation in the studied population. They noticed no significant differences in either the mild or severe CoA groups for any anatomic characteristics.

In our study, it was found that coarctation area indexed to BSA is the most important feature with sensitivity 95.65%, specificity 92.86% and AUC of 0.994 with cut off value ≤23.8 mm^2, this came in agreement with echocardiography based classification and all patients were classified correctly, This was in line with Nielsen's [25] findings according to which the parameters with the biggest area under the ROC curve were those with the lowest aorta cross-sectional area indexed to the area of the body's surface.

Using coarctation diameter indexed to patient height, it revealed sensitivity 95.65%, specificity 78.57% and AUC of 0.972 with cut off value ≤ 0.05mm, out of 14 cases of mild group 3 cases had no agreement between echocardiography and MSCT in determining the degree of severity, which is different from Yu., *et al*., [8] results that showed that CoA diameter indexed to height was an optimal feature for classifying the severity of CoA.

While using coarctation diameter indexed to patient weight it revealed sensitivity 91.30%, specificity 85.71% and AUC of 0.891 with cut off value ≤ 0.66mm, two cases out of 14 cases of mild group, and two cases out of 23 cases of severe group had no agreement between echocardiography and MSCT in determining the degree of severity.

As regard coarctation diameter indexed to descending aorta diameter, Zhao Q, *et al*., [26] classified patients with CoA according to severity of coarctation based on the ratio of the aortic diameter at the coarctation site to that at the diaphragm (coarctation site–diaphragm ratio, CDR) into two groups: mild group (CDR > 50%) and severe group (CDR < 50%). In our study out of 14 cases of mild group 2 cases had no agreement with Zhao. Q [26] results.

Limitations: The sample size was relatively small and lacked follow-up after coarctation repair. The reliability of the severity of aortic coarctation assessments may be reduced by the precision of the pressure gradient determined from echocardiography.

Conclusions

The anatomical characteristics derived from computed tomography angiography can assess the extent of aortic coarctation, suggesting that it is important to take into account both the anatomical alterations at the CoA sites and the patient's development.

Financial support and sponsorship: Nil
Conflict of Interest: Nil

Acknowledgements
The authors thank all the study participants for their patience and support.

Funding: This study had no funding from any resource.

Availability of data and materials: The data supporting the conclusions of this article are available upon reasonable request from the authors.

Declarations
Ethics approval and consent to participate
Consent for publication: Not applicable.

Competing interests: The authors declare they have no competing interests.

References

1. Liu Y, Chen S, Zühlke L, Black GC, Choy MK, Li N, *et al*. Global birth prevalence of congenital heart defects 1970-2017: updated systematic review and meta-analysis of 260 studies. Int J Epidemiol. 2019;48:455-63.
2. van der Linde D, Konings EE, Slager MA, Witsenburg M, Helbing WA, Takkenberg JJ, *et al*. Birth prevalence of congenital heart disease worldwide: a systematic review and meta-analysis. J Am Coll Cardiol. 2011;58:2241-7.
3. Eichhorn JG, Ley S, Kropp F, Fink C, Brockmeier K, Loukanov T, *et al*. Aortic Coarctation a Systemic Vessel Disease-Insights from Magnetic Resonance Imaging. Thorac Cardiovasc Surg. 2019;67:e1-e10.
4. Swanson L, Owen B, Keshmiri A, Deyranlou A, Aldersley T, Lawrenson J, *et al*. A Patient-Specific CFD Pipeline Using Doppler Echocardiography for Application in Coarctation of the Aorta in a Limited Resource Clinical Context. Front Bioeng Biotechnol. 2020;8:409.
5. Shi Y, Valverde I, Lawford PV, Beerbaum P, Hose DR. Patient-specific non-invasive estimation of pressure gradient across aortic coarctation using magnetic resonance imaging. J Cardiol. 2019;73:544-52.
6. Jurcut R, Daraban AM, Lorber A, Deleanu D, Amzulescu MS, Zara C, *et al*. Coarctation of the aorta in adults: what is the best treatment? Case report and literature review. J Med Life. 2011;4:189-95.
7. Bigdelian H, Sedighi M. Repair of aortic coarctation in infancy: A 10-year clinical experience. Asian Cardiovasc Thorac Ann. 2016;24:417-21.
8. Yu Y, Wang Y, Yang M, Huang M, Li J, Jia Q, *et al*. Evaluating the severity of aortic coarctation in infants using anatomic features measured on CTA. Eur Radiol. 2021;31:1216-26.
9. Pepe M, Iacovelli F, Masi F, Marangelli V, Scardapane A, De Santis A, *et al*. Aortic coarctation: guidelines mismatch across the ocean. Journal of Cardiothoracic Surgery. 2014;9:38.
10. Trattner S, Chelliah A, Prinsen P, Ruzal-Shapiro CB, Xu Y, Jambawalikar S, *et al*. Estimating Effective Dose

of Radiation From Pediatric Cardiac CT Angiography Using a 64-MDCT Scanner: New Conversion Factors Relating Dose-Length Product to Effective Dose. AJR Am J Roentgenol. 2017;208:585-94.
11. Bernard A, Comby PO, Lemogne B, Haioun K, Ricolfi F, Chevallier O, *et al*. Deep learning reconstruction versus iterative reconstruction for cardiac CT angiography in a stroke imaging protocol: Reduced radiation dose and improved image quality. Quant Imaging Med Surg. 2021;11:392-401.
12. Sabarudin A, Siong TW, Chin AW, Hoong NK, Karim MKA. A comparison study of radiation effective dose in ECG-Gated Coronary CT Angiography and calcium scoring examinations performed with a dual-source CT scanner. Sci Rep. 2019;9:4374.
13. Koplay M, Kizilca O, Cimen D, Sivri M, Erdogan H, Guvenc O, *et al*. Prospective ECG-gated high-pitch dual-source cardiac CT angiography in the diagnosis of congenital cardiovascular abnormalities: Radiation dose and diagnostic efficacy in a pediatric population. Diagn Interv Imaging. 2016;97:1141-50.
14. Huang F, Chen Q, Huang WH, Wu H, Li WC, Lai QQ, *et al*. Diagnosis of Congenital Coarctation of the Aorta and Accompany Malformations in Infants by Multi-Detector Computed Tomography Angiography and Transthoracic Echocardiography: A Chinese Clinical Study. Med Sci Monit. 2017;23:2308-14.
15. Shehata S, Zaiton F, Warda MA, Shahbah D, Ebrahim B. Value of MDCT as a non-invasive modality in evaluation of pediatric congenital cardiovascular anomalies. Egypt J Radiol Nucl Med. 2017;48:467-78.
16. Chandrashekhar G, Sodhi KS, Saxena AK, Rohit MK, Khandelwal N. Correlation of 64 row MDCT, echocardiography and cardiac catheterization angiography in assessment of pulmonary arterial anatomy in children with cyanotic congenital heart disease. Eur J Radiol. 2012;81:4211-7.
17. Omnia AK, Ahmed MM. Role of multidetector computed tomography (MDCT) angiography in preoperative assessment of coarctation of the aorta in pediatric patients and young adults. Egypt J Radiol Nucl Med. 2011;42:297-303.
18. Goo HW. State-of-the-art CT imaging techniques for congenital heart disease. Korean J Radiol. 2010;11:4-18.
19. Kim ER, Kim WH, Nam J, Choi K, Jang WS, Kwak JG, *et al*. Mid-Term Outcomes of Repair of Coarctation of Aorta with Hypoplastic Arch: Extended End-to-side Anastomosis Technique. Semin Thorac Cardiovasc Surg. 2017:112-15.
20. Sendzikaite S, Sudikiene R, Tarutis V, Lubaua I, Silis P, Rybak A, *et al*. Prevalence of arterial hypertension, hemodynamic phenotypes, and left ventricular hypertrophy in children after coarctation repair: A multicenter cross-sectional study. Pediatr Nephrol. 2020;35:2147-55.
21. Wu Y, Li J, Wu C, Zhu J, He L, Feng C, *et al*. Diagnosis and surgical repair for coarctation of the aorta with intracardiac defects: A single center experience based on 93 infants. Front Pediatr. 2020;8:49-52.
22. Dijkema EJ, Dik L, Breur JMP, Sieswerda GT, Haas F, Slieker MG, *et al*. Two decades of aortic coarctation treatment in children; evaluating techniques. Neth Heart J. 2021;29:98-104.
23. Zhao Q, Shi K, Yang ZG, Diao KY, Xu HY, Liu X, *et al*. Predictors of aortic dilation in patients with coarctation of the aorta: evaluation with dual-source computed tomography. BMC Cardiovasc Disord. 2018;18:124.
24. Teo LL, Cannell T, Babu-Narayan SV, Hughes M, Mohiaddin RH. Prevalence of associated cardiovascular abnormalities in 500 patients with aortic coarctation referred for cardiovascular magnetic resonance imaging to a tertiary center. Pediatr Cardiol. 2011;32:1120-7.
25. Nielsen JC, Powell AJ, Gauvreau K, Marcus EN, Prakash A, Geva T, *et al*. Magnetic resonance imaging predictors of coarctation severity. Circulation. 2005;111:622-8.
26. Zhao Q, Wang J, Yang ZG, Shi K, Diao KY, Huang S, *et al*. Assessment of intracardiac and extracardiac anomalies associated with coarctation of aorta and interrupted aortic arch using dual-source computed tomography. Sci. Rep. 2019;9:11656.

How to Cite This Article
Abdelmaksoud AM, Mohamad DM, Dawoud RM, Hablas LT. Diagnostic efficiency of anatomic features measured by 320- slice multi-detector computed tomography angiography in evaluating the severity of aortic coarctation. International Journal of Radiology and Diagnostic Imaging. 2023; 6(3): 123-132.